A nonsense mutation in *TFEC* is the likely cause of the recessive piebald phenotype in ball pythons (*Python regius*)

*Alan Garcia-Elfring, Heather L. Roffey, *Andrew P. Hendry, and *Rowan D. H. Barrett

*Redpath Museum and Department of Biology, McGill University, Montreal, QC, Canada

The corresponding author's email address: alan.garcia-elfring@mail.mcgill.ca

Abstract

Captive-bred ball pythons (*Python regius*) represent a powerful model system for studying the genetic basis of colour variation and Mendelian phenotypes in vertebrates. Although hundreds of Mendelian phenotypes (colour morphs) affecting colouration and patterning have been described for ball pythons, the genes causing these colour morphs remain unknown. Here, we used crowdsourcing of samples from commercial ball python breeders to investigate the genetic basis of a classic phenotype found in the pet trade, the piebald [characterized by dorsolateral patches of unpigmented (white) skin]. We used whole-genome sequencing of pooled samples followed by population genetic methods to delineate the genomic region containing the causal gene. We identified *TFEC* of the MIT-family of transcription factors as a candidate gene. Functional annotation of SNPs identified a nonsense mutation in *TFEC*, which we conclude is the likely causal variant for the piebald phenotype. Our work shows that ball python colour morphs have the potential to be an excellent model system for studying the genetic basis of pigment variation in vertebrates, and highlights how collaborations with commercial breeders can accelerate discoveries.

33 **Introduction**

34 The study of colour variation has a long history in evolutionary biology and genetics (Caro 2017;
35 Cuthill et al. 2017; Harris et al. 2019). Over 150 years ago, crossing yellow and green peas
36 helped Mendel to discover that traits are inherited as discrete hereditary units or "factors"
37 (Mendel 1866; reviewed by Ellis et al. 2011). Once Mendel's work was rediscovered in 1900,
38 invertebrate colour variation helped establish that Mendel's "factors", which we now call
39 genes, were located on chromosomes (Bridges 1919; Harrison 1920). Further, colour variation
40 in vertebrates has provided insights in many fields, particularly the biomedical sciences (e.g.
41 Pingault et al. 1998; Tachibana et al. 2003; Richards et al. 2019), developmental biology (e.g.
42 Cohen et al. 2016; Haupaix et al. 2018), and evolutionary biology (e.g. Schweizer et al. 2018;
43 Barrett et al. 2019; Burgon et al. 2020; reviewed by San-Jose and Roulin 2017). However, our
44 current knowledge of the genetics of vertebrate colouration comes primarily from studies on
45 model species, particularly the mouse (e.g. Baxter et al. 2004; Hoekstra 2006; San-Jose and
46 Roulin 2017; but see Ullate-Agote et al. 2020). This bias in the literature provides a limited view
47 of the ways in which genetic variation can affect vertebrate colouration.

48 Although mice, as all mammals and birds, have one pigment-producing cell type
49 (melanocytes) which synthesizes melanin, reptiles, like fish and amphibians, have three colour-
50 producing cells or chromatophores (reviewed by Bechtel 1978; Mills and Patterson 2009;
51 Olsson et al. 2013). In addition to melanin-producing cells, called melanophores, reptiles have
52 xanthophores and iridiophores that contribute to colouration. Xanthphores synthesize yellow
53 pteridine-based pigments and can also contain red carotenoid pigments that are obtained from

54 diet (often called erythrophores). Iridiophores do not contain pigments but instead produce
55 structural colouration by reflecting light on guanine nanocrystals (Teyssier et al. 2015). The
56 three colour-producing cells interact in 3D space (Grether et al. 2004; Saenko et al. 2013) to
57 generate the remarkable range of colour variation observed in reptiles.

58 We propose that the ball python (*Python regius*; Figure 1a) is an excellent model for
59 studying the genetic basis of vertebrate colouration (Irizarry and Bryden 2016). Ball pythons are
60 native to western Sub-Saharan Africa, with a range extending from Senegal to Uganda. With a
61 maximum length of approximately 6 feet long, ball pythons are small relative to their better-
62 known Asian congener, the Burmese python (*Python bivittatus*). Owing to their small size,
63 docility, and simple husbandry, ball pythons rose in popularity in the pet trade, particularly
64 among reptile enthusiasts. An additional factor that has contributed to the ball python's
65 popularity was the discovery of rare phenotypes that affect colouration. In Ghana, claims of
66 rare wild ball pythons with altered patterning go back as early as 1966. In the early 1990s, one
67 such ball python was caught, a piebald. This individual had patches of unpigmented (white) skin
68 (e.g. Figure 1b-d), a pigment deficiency found in many vertebrates (Ahi and Sefc 2017),
69 including humans (Oiso et al. 2013). However, it would take a few years to rule out
70 environmental factors as a causal explanation for the piebald phenotype in the ball python
71 caught from the wild. By 1998, Peter Kahl had reproduced the piebald phenotype in captivity
72 (called 'proving' by commercial breeders) and showed it had a recessive mode of inheritance (*A*
73 *brief history of Royal Ball Python morphs for beginners*, n.d.). This pioneering work of breeders
74 and hobbyists spurred the discovery and propagation of numerous additional and highly diverse
75 colour morphs (e.g. Figure 1b-g). Today, 314 Mendelian phenotypes (i.e., phenotypes that

76 segregate as a single Mendelian factor or major quantitative trait locus) are bred in captivity
77 (known as 'basic' morphs; http://www.worldofballpythons.com/morphs), providing a valuable
78 resource for studying the genetics of vertebrate colouration in great detail. Indeed, commercial
79 breeders have taken advantage of epistasis and produced over 6000 unique phenotypes
80 ('designer morphs') with different combinations of the Mendelian colour factors.

81 Ball pythons therefore provide an outstanding opportunity to study the genetic basis of
82 Mendelian phenotypes related to pigmentation and patterning. For example, ball python colour
83 morphs can be characterized by changes to pattern or to pigmentation or both. Phenotypes
84 with changes to pigmentation but not pattern (Figure 1c) are presumably determined by
85 changes to genes with roles in a pigment synthesis pathway. On the other hand, aberrations to
86 pattern, like white-spotting, are thought to occur through mutations in genes with functions in
87 progenitor cell migration and differentiation from the neural crest (reviewed by Mills and
88 Patterson 2009). However, most research on colouration, vertebrate and invertebrate, has
89 focused on pigmentation, particularly melanin-based pigmentation (e.g. San-Jose and Roulin
90 2018), rather than on patterning (Mills and Patterson 2009). The extensive phenotypic variation
91 in pigment and pattern found in captive-bred ball pythons can therefore help correct the bias
92 (e.g. Ullate-Agote et al. 2020) associated with mammalian models and melanin-based
93 pigmentation in the scientific literature on vertebrate colouration.

94 In this study, our goal was to discover the candidate mutation(s) that produce the
95 Mendelian phenotype affecting pattern in ball pythons, the piebald (Figure 1b). We used
96 crowdsourcing of samples from commercial breeders, thereby bridging a gap between

97 academia and industry. Genes known to cause white-spotting in other vertebrates, like *KIT,*
98 *MITF*, *EDNRB*, and *SOX10* (Fleischman et al. 1991; Baxter et al. 2004; Ahi and Sefc 2017)
99 represent *a priori* candidate genes, but given the differences in pigmentation development
100 between reptiles and previously studied model systems, we employed a whole-genome
101 approach to facilitate discovery of unknown candidate genes. We sequenced whole-genomes of
102 pooled samples and then applied population genetic methods to delineate the genomic region
103 of interest and identify candidate genes. We then functionally annotated SNPs to identify the
104 putative causal mutation. Given the character of the piebald phenotype (i.e., dorsolateral
105 patches of unpigmented skin), we expected the candidate gene to be expressed in the neural
106 crest and associated with chromatophore migration and differentiation.

107

108 **Methods**

109 *Sampling and DNA extraction*

110 We obtained ball python samples by crowd-sourcing from commercial breeders in Canada
111 (Mutation Creation, T. Dot Exotics, The Ball Room Canada, Designing Morphs), who supplied us
112 with shed skin. We then used shed skin samples for 47 piebald individuals (i.e., individuals
113 homozygous for the piebald variant; Table S1) and 52 non-piebald individuals (Table S2).
114 Although individuals from both sets of samples contained additional basic morphs, the only
115 consistent difference between the two was the piebald phenotype. We attempted to maximize
116 the number of individuals that come from different families to minimize the effects of
117 population structure, although there were some exceptions (Table S2). From each sample we

118 used approximately 0.1 g of shed skin, cut to small pieces using scissors, for DNA extraction. We
119 extracted DNA following a standard phenol-chloroform procedure, with a 24-hour proteinase-K
120 incubation time at 37 °C. Piebald and non-piebald samples were prepared on different working
121 days to avoid contamination. We quantified all samples using a Picogreen® ds DNA assay
122 (Thermo Fisher Scientific, Waltham, USA) on an Infinite® 200 Nanoquant (Tecan Group Ltd.
123 Männedorf, Switzerland).

124 *Sequencing*

125 After DNA extraction, we mixed DNA of individuals (according to phenotype) in equimolar
126 amounts to obtain a single pool for each phenotype, 'piebald' and 'non-piebald.' We used PCR-
127 based whole-genome libraries for both pools, which were prepared at the McGill University and
128 Genome Quebec Innovation Center, Montreal, Canada. We sequenced 150 bp paired-end reads
129 using two lanes of Illumina HiSeqX.

130 *Bioinformatics*

131 To process raw reads, we applied filters based on read quality and length, keeping reads with a
132 minimum quality of 20 (--quality-threshold 20) and a length of 50 bp (--min-length 50). We then
133 aligned processed reads to the Burmese python (*Python bivittatus*) draft assembly Pmo2.0
134 (Castoe et al. 2013) using the program *NextGenMap* (Sedlazeck et al. 2013). *NextGenMap* was
135 designed for aligning reads to highly polymorphic genomes or genomes of closely related
136 species. We used *SAMtools* (Li et al. 2009) to convert SAM files to BAM format and remove
137 reads with mapping quality below 20 (samtools view -q 20). We filtered for PCR duplicates using
138 the program *MarkDuplicates* of Picard Tools (Wysoker et al. 2013). We then created a mpileup

139 file (samtools mpilep -B) from which the synchronized (sync) file was produced using
140 *Popoolation2* (Kofler et al. 2011b). The sync file contains read counts for all nucleotides
141 sequenced in the genome and it is used for subsequent downstream analyses (e.g. F_{ST} scan).
142 We also applied the same protocol as above but instead aligned reads to the chromosome-
143 length Burmese python reference genome, Python_molurus_bivittatus-5.0.2_HiC.assembly
144 (Dudchenko et al. 2017, 2018).

145 *Identification of fixed SNPs and delineation of the candidate genomic region*

146 We applied an F_{ST} scan to identify fixed SNPs across the two pools. For this procedure, we used
147 the *fst-sliding.pl* script of *Popoolation2* (--min-count 10, --min-coverage 20, --max-coverage 500,
148 --min-covered-fraction 0, --window-size 1, --step-size 1, --pool-size 47:52, --suppress-
149 noninformative). We then identified candidate SNPs as those with F_{ST} estimates of 1 and
150 mapped them to genes. We used a custom BASH script to map fixed SNPs to genes in the gene
151 annotation file using scaffold and SNP position. Because the draft assembly is highly
152 fragmented (Castoe et al. 2013), we also applied the same F_{ST} scan on data aligned to the
153 chromosome-length genome assembly (Dudchenko et al. 2017, 2018) to get a better
154 delineation of the genomic region of interest within candidate SNPs. However, this latter
155 assembly is not annotated with genetic features – hence necessitating the use of both
156 assemblies.

157 *Functional annotation of SNPs*

158 We next functionally annotated genome-wide SNPs with the software snpEff (Cingolani et al.
159 2012) to aid in identifying the putative causal mutation for the piebald phenotype. SnpEff was

160 designed for annotating and predicting the effects of SNPs, such as amino acid changes. This
161 program provides an assessment of the impact of a SNP, including 'HIGH' (e.g. stop codon),
162 'MODERATE' (e.g. non-synonymous change), 'LOW' (e.g. synonymous change), or 'MODIFIER'
163 (change in an intergenic area).

164

165 **Results**

166 *SNP dataset*

167 From the BAM files, we obtained an average depth of coverage of 50.5 and 52.6 for the piebald
168 and non-piebald pools, respectively. After filtering, our dataset consisted of 3,095,304 SNPs for
169 the draft assembly and 3,221,285 SNPs in the chromosome-length assembly.

170 *FST scan for fixed SNPs and candidate genomic region*

171 Across all SNPs, we found an average F_{ST} of 0.03456 – relatively low, indicating that population
172 structure was minimized. Using the draft assembly, we identified 129 fixed SNPs (F_{ST} = 1.0) and
173 369 SNPs with F_{ST} > 0.9. Plotting the F_{ST} values (Figure S1) shows peaks across the reference
174 genome, demonstrating the fragmented state of the draft assembly. In the chromosome-length
175 assembly, we found 131 fixed SNPs (F_{ST} = 1.0) and 372 SNPs with F_{ST} > 0.9. The chromosome-
176 length assembly also shows that 128/131 fixed SNPs and 365/372 SNPs with F_{ST} > 0.9 map to a
177 single region on scaffold 7, clearly delineating a genomic region of interest (Figure 2). The 128
178 fixed SNPs map to a region 8 Mb long (scaffold 7: 49526089-57612101). This region becomes
179 26.5 Mb when considering the 365 SNPs with F_{ST} > 0.9 (scaffold 7: 49246858-76754467).

180 However, most of these 365 SNPs cluster within the 8 Mb region demarcated by fixed SNPs,
181 with only 11 mapping beyond the bounds of this region (three upstream, eight downstream).

182 *Candidate genes and SNP annotation*

183 We found that 59 fixed SNPs map to 12 different protein-coding genes (*BMT2*, *CAPZA2*, *CNTN1*,
184 *DOCK4*, *FOXP2*, *GPR85*, *KCND2*, *LOC103067393*, *LSMEM1*, *ST7*, *TES*, and *TFEC*). We annotated
185 SNPs for predicted impact (see methods) and found that all fixed SNPs have the lowest impact
186 classification (MODIFIER), often assigned to mutations in non-functional regions, and most map
187 to introns. However, we found other impact classifications among SNPs with F_{ST} greater than
188 0.9. One synonymous (i.e., silent) SNP (LOW impact, NW_006539084.1 26867, F_{ST} = 0.92) is
189 located within the gene *LSMEM1* and one nonsense SNP (HIGH impact, NW_006534020.1
190 160458, F_{ST} = 0.96) is located within the gene *TFEC*. This nonsense variant consisted of a C>T
191 mutation on Arg165, resulting in a premature Opal stop codon (Table S3).

192

193 **Discussion**

194 We regard the ball python as a powerful new model for understanding the genetic basis of
195 pigmentation in vertebrates. As proof-of-principle, we set out to discover candidate genes and
196 causal mutations for the classic colour morph found in the pet trade, the piebald. Over the last
197 thirty years, ball python breeders have discovered and successfully propagated in captivity
198 more than three hundred Mendelian phenotypes. Yet, researchers working on the genetics of
199 vertebrate colouration have been slow to appreciate the ball python as a powerful new model

200 (but see Irizarry and Bryden 2016). We set out to bridge this gap. To do so, we appealed to
201 commercial ball python breeders to join our efforts in discovery, starting with uncovering the
202 genetic basis of the piebald phenotype. Commercial breeders have a vested interest in
203 acquiring the ability to identify heterozygotes for recessive phenotypes (i.e., carriers of
204 recessive alleles affecting colouration), and piebald is one such phenotype, although subtle
205 phenotypic differences on heterozygotes are not uncommon (e.g. ring of unpigmented skin,
206 often near the vent).

207 To elucidate the genetic basis of the piebald phenotype, we combined a case-control
208 experimental design with whole-genome sequencing, population genetic methods, and
209 functional annotation of the candidate SNPs. We identified a premature stop codon in the
210 protein-coding region of the gene *TFEC* as the putative genetic basis for this Mendelian
211 phenotype. *TFEC* belongs to a family of transcription factors (*MITF*) known to be expressed in
212 the neural crest and pigment cells. However, functional validation through gene editing
213 techniques, like CRISPR cas9 (Rasys et al. 2019), is required to establish that the candidate
214 nonsense mutation is the causal variant.

215 With knowledge of the specific genetic variants underlying pigmentation variation in ball
216 pythons, gene editing could pave the way to produce colour morphs free of secondary
217 phenotypes that are undesired from a commercial or ethical perspective. Genes that contribute
218 to colouration are also expressed in many other tissues derived from neural crest cells
219 (Donoghue et al. 2008). Thus, mutations that alter colour or patterning often alter other traits,
220 such as behaviour (Ducrest et al. 2008; McKinnon and Pierotti 2010). Not surprisingly, there are

221 ball python colour morphs linked to morphological deformities and neurological dysfunction
222 (Rose and Williams 2014). For example, the incomplete dominant 'spider' morph is associated
223 with a neurological syndrome called the 'head wobble' (Fox and Hogan 2020). The propagation
224 of colour morphs with correlated traits have implications for the health and welfare of ball
225 pythons in captivity (Rose and Williams 2014) and are a source of current controversy among
226 hobbyists and commercial breeders (Riera 2015). In 2017, the International Herpetological
227 Society in the U. K. banned ball pythons with the spider mutation, which is thought to be
228 homozygous lethal, from their reptile shows (International Herpetological Society 2020).
229 However, it is not known if the correlated trait(s) for any particular colour morph is due to
230 pleiotropic effects or linked variation. If due to linked variation, targeted mutation on a
231 different genetic background (i.e., without the linked variant) could allow the reproduction of
232 colour phenotypes free of behavioural and morphological abnormalities. If due to pleiotropy,
233 targeted mutation at different nearby loci could achieve the same effect.

234 The wide variety of ball python phenotypes found in the pet trade offers the
235 opportunity to study how genes control vertebrate pigmentation and pattern formation.
236 Changes to pigmentation are often caused by mutations in genes involved in the pigment
237 synthesis pathway (Mills and Patterson 2009; Hubbard et al. 2010). For example, albinism
238 occurs when an individual inherits two copies of a gene involved in melanin synthesis (e.g.
239 OCA2) that is non-functional. Snakes with two non-functional OCA2 genes lack dark melanin-
240 based pigment though contain yellow pigments produced in the xanthophores (Saenko et al.
241 2015). Changes to pattern, on the other hand, are often attributed to genes with functions in
242 cell migration from the neural crest and differentiation into colour-producing cells (Mills and

243 Patterson 2009). However, Mendelian phenotypes characterized by changes to either
244 pigmentation or patterning are likely to map to the protein-coding regions of genes. Genomic
245 research on the most extensively studied vertebrate, humans, shows that Mendelian
246 phenotypes are generally caused by mutations arising in protein-coding regions and affecting
247 protein function (Cooper et al. 2010; Chong et al. 2015). The progenitor cells of
248 chromatophores originate in the neural crest and mutations to these genes result in partial or
249 total loss of pigment and structural colouration. Mutations to genes such as *MITF*, *KIT*, *EDNRB*,
250 and *SOX10*, which are expressed in the neural crest, results in white spotting or a complete lack
251 of pigment across a wide range of vertebrates, including fish, amphibians, birds, and mammals
252 (Baxter et al. 2004; Kelsh 2006; George et al. 2016; Ahi and Sefc 2017; Woodcock et al. 2017;
253 Camargo-Sosa et al. 2019; Goding and Arnheiter 2019). These genes represented *a priori*
254 candidates for the piebald phenotype in ball pythons, but did not show differentiation between
255 our phenotypic pools.

256 We identified a putative causal mutation for the piebald phenotype in ball pythons
257 located in a new candidate gene for vertebrate pigmentation: the gene *TFEC* (Figure 3, Table
258 S3). This variant, which produces a premature stop codon, was nearly fixed (F_{ST} = 0.96).
259 Complete differentiation between the piebald and non-piebald pools was prevented by a single
260 read for the reference allele that was sequenced in the piebald samples. It is possible this is the
261 result of a sequencing error or the inclusion of an unknown heterozygote. *TFEC* was not one of
262 the candidate genes expected *a priori*. This particular gene has not been implicated in
263 mammalian colouration. However, *TFEC* is part of the MIT-family of transcription factors known
264 to be involved in animal patterning. For example, this family consists of the gene *MITF*, which

265 forms heterodimers with the other three members, *TFEB*, *TFE3*, and *TFEC* (Goding and
266 Arnheiter 2019). In mouse models, double knockout mutations to *MITF* and *TFE3* cause all-
267 white phenotypes (Steingrímsson et al. 2002). Interestingly, the same study showed that
268 knocking out *TFEC* did not result in a phenotype different from the wild-type mouse. There is
269 evidence that shows *TFEC* is expressed in the retinal pigment epithelium of mammals (Rowan et
270 al. 2004). No evidence suggests, however, that *TFEC* is expressed in cells that descend from the
271 mammalian neural crest, which includes pigment-producing cells. In contrast, recent evidence
272 from the zebrafish model shows that *TFEC* is highly expressed in neural crest cells, specifically
273 progenitor pigment cells and iridophores (Petratou et al. 2019; Saunders et al. 2019). In fact,
274 *TFEC* is expressed in two dorsolateral patches on the torso during embryogenesis (Lister et al.
275 2011; Petratou et al. 2018; Petratou et al. 2019), reminiscent of where the white-spotting
276 occurs in the piebald phenotype in ball pythons. The expression patterns of *TFEC* in zebrafish,
277 together with our results, makes a strong case that *TFEC* is the piebald gene in ball pythons and
278 that a premature stop codon is the likely causal mutation.

279

280 **Conclusion**

281 In this study, we aimed to uncover, for the first time, the genetic basis of a ball python colour
282 morph. We discovered that a premature stop codon in the gene *TFEC* is the likely cause for the
283 Mendelian piebald phenotype found in ball pythons from the pet trade. The lack of evidence for
284 *TFEC* affecting mammalian pigmentation highlights the need to study the genetic basis of
285 colouration in non-mammalian vertebrate models. Future work will be aimed at demonstrating

causality through direct functional manipulation. These efforts would produce the first genetically engineered ball python, a step that would open the door to safe reproduction of other colour morphs through targeted mutation.

Acknowledgments

RDHB was supported by an NSERC Discovery Grant and Canada Research Chair. We thank Mutation Creation, T Dot Exotics, The Ball Room Canada, and Designing Morphs for supplying samples.

Data accessibility

The data that support the findings of this manuscript will be uploaded to Dryad.

Contributions

AGE, HR, APH, and RDHB conceived and designed the study. HR collected samples. AGE performed the molecular work. AGE performed the bioinformatics and analyzed the genomic data. AGE wrote the manuscript with input from all authors.

REFERENCES

304 Ahi, E.P. and Sefc, K.M., 2017. A gene expression study of dorso-ventrally restricted pigment
305 pattern in adult fins of Neolamprologus meeli, an African cichlid species. PeerJ, 5,
306 p.e2843.

307 Barrett, R.D., Laurent, S., Mallarino, R., Pfeifer, S.P., Xu, C.C., Foll, M., Wakamatsu, K., Duke-
308 Cohan, J.S., Jensen, J.D. and Hoekstra, H.E., 2019. Linking a mutation to survival in wild
309 mice. Science, 363(6426), pp

310 Baxter, L.L., Hou, L., Loftus, S.K. and Pavan, W.J., 2004. Spotlight on spotted mice: a review of
311 white spotting mouse mutants and associated human pigmentation disorders. Pigment
312 Cell Research, 17(3), pp.215-224..499-504.

313 Bechtel, H.B., 1978. Color and pattern in snakes (Reptilia, Serpentes). Journal of Herpetology,
314 pp.521-532.

315 Bridges, C.B., 1919. The genetics of purple eye color in Drosophila. Journal of Experimental
316 Zoology, 28(2), pp.265-305.

317 A brief history of Royal Ball Python morphs for beginners. Retrieved from
318 http://bagnallsreptiles.weebly.com/history-into-morphs.html

319 Burgon, J.D., Vieites, D.R., Jacobs, A., Weidt, S.K., Gunter, H.M., Steinfartz, S., Burgess, K.,
320 Mable, B.K. and Elmer, K.R., 2020. Functional colour genes and signals of selection in
321 colour-polymorphic salamanders. Molecular ecology, 29(7), pp.1284-1299.

322 Camargo-Sosa, K., Colanesi, S., Müller, J., Schulte-Merker, S., Stemple, D., Patton, E.E. and
323 Kelsh, R.N., 2019. Endothelin receptor Aa regulates proliferation and differentiation of
324 Erb-dependent pigment progenitors in zebrafish. PLoS genetics, 15(2), p.e1007941.

325 Caro, T., 2017. Wallace on coloration: contemporary perspective and unresolved insights.
326 Trends in ecology & evolution, 32(1), pp.23-30.

327 Castoe, T.A., de Koning, A.J., Hall, K.T., Card, D.C., Schield, D.R., Fujita, M.K., Ruggiero, R.P.,
328 Degner, J.F., Daza, J.M., Gu, W. and Reyes-Velasco, J., 2013. The Burmese python
329 genome reveals the molecular basis for extreme adaptation in snakes. Proceedings of
330 the National Academy of Sciences, 110(51), pp.20645-20650.

331 Chong, J.X., Buckingham, K.J., Jhangiani, S.N., Boehm, C., Sobreira, N., Smith, J.D., Harrell, T.M.,
332 McMillin, M.J., Wiszniewski, W., Gambin, T. and Akdemir, Z.H.C., 2015. The genetic basis
333 of Mendelian phenotypes: discoveries, challenges, and opportunities. The American
334 Journal of Human Genetics, 97(2), pp.199-215.

335 Cingolani, P., Platts, A., Wang, L.L., Coon, M., Nguyen, T., Wang, L., Land, S.J., Lu, X. and Ruden,
336 D.M., 2012. A program for annotating and predicting the effects of single nucleotide
337 polymorphisms, SnpEff: SNPs in the genome of Drosophila melanogaster strain w1118;
338 iso-2; iso-3. Fly, 6(2), pp.80-92.

339 Cohen, M.A., Wert, K.J., Goldmann, J., Markoulaki, S., Buganim, Y., Fu, D. and Jaenisch, R., 2016.
340 Human neural crest cells contribute to coat pigmentation in interspecies chimeras after
341 in utero injection into mouse embryos. Proceedings of the National Academy of
342 Sciences, 113(6), pp.1570-1575.

343 Cooper, D.N., Chen, J.M., Ball, E.V., Howells, K., Mort, M., Phillips, A.D., Chuzhanova, N.,
344 Krawczak, M., Kehrer-Sawatzki, H. and Stenson, P.D., 2010. Genes, mutations, and
345 human inherited disease at the dawn of the age of personalized genomics. Human
346 mutation, 31(6), pp.631-655.

347 Cuthill, I.C., Allen, W.L., Arbuckle, K., Caspers, B., Chaplin, G., Hauber, M.E., Hill, G.E., Jablonski,
348 N.G., Jiggins, C.D., Kelber, A. and Mappes, J., 2017. The biology of color. Science,
349 357(6350), p.eaan0221.

350 Donoghue, P.C., Graham, A. and Kelsh, R.N., 2008. The origin and evolution of the neural crest.
351 Bioessays, 30(6), pp.530-541.

352 Ducrest, A.L., Keller, L. and Roulin, A., 2008. Pleiotropy in the melanocortin system, coloration
353 and behavioural syndromes. Trends in ecology & evolution, 23(9), pp.502-510.

354 Dudchenko, O., Batra, S.S., Omer, A.D., Nyquist, S.K., Hoeger, M., Durand, N.C., Shamim, M.S.,
355 Machol, I., Lander, E.S., Aiden, A.P. and Aiden, E.L., 2017. De novo assembly of the
356 Aedes aegypti genome using Hi-C yields chromosome-length scaffolds. Science,
357 356(6333), pp.92-95.

358 Dudchenko, O., Shamim, M.S., Batra, S., Durand, N.C., Musial, N.T., Mostofa, R., Pham, M.,
359 Hilaire, B.G.S., Yao, W., Stamenova, E., Hoeger, M., Nyquist, S.K., Korchina, V., Pletch, K.,
360 Flanagan, J.P., Tomaszewicz, A., McAloose, D., Estrada, C.P., Novak, B.J., Omer, A.D.,
361 Aiden, E.L., 2018. The Juicebox Assembly Tools module facilitates de novo assembly of
362 mammalian genomes with chromosome-length scaffolds for under $1000. bioRxiv
363 254797. https://doi.org/10.1101/254797.

364 Ellis, T.N., Hofer, J.M., Timmerman-Vaughan, G.M., Coyne, C.J. and Hellens, R.P., 2011. Mendel,
365 150 years on. Trends in plant science, 16(11), pp.590-596.

366 Fleischman, R.A., Saltman, D.L., Stastny, V. and Zneimer, S., 1991. Deletion of the c-kit
367 protooncogene in the human developmental defect piebald trait. Proceedings of the
368 National Academy of Sciences, 88(23), pp.10885-10889.

369 Fox, B.C. and Hogan, S., 2020. Hypopigmentation as the Cause for the Neurological Disorder
370 "Spider Wobble" in Python regius.

371 George, A., Zand, D.J., Hufnagel, R.B., Sharma, R., Sergeev, Y.V., Legare, J.M., Rice, G.M.,
372 Schwoerer, J.A.S., Rius, M., Tetri, L. and Gamm, D.M., 2016. Biallelic mutations in MITF
373 cause coloboma, osteopetrosis, microphthalmia, macrocephaly, albinism, and deafness.
374 The American Journal of Human Genetics, 99(6), pp.1388-1394.

375 Goding, C.R. and Arnheiter, H., 2019. MITF—the first 25 years. Genes & development, 33(15-
376 16), pp.983-1007.

377 Grether, G.F., Kolluru, G.R. and Nersissian, K., 2004. Individual colour patches as
378 multicomponent signals. Biological Reviews, 79(3), pp.583-610.

379 Harris RB, Irwin K, Jones MR, Laurent S, Barrett RD, Nachman MW, Good JM, Linnen CR, Jensen
380 JD, Pfeifer SP. The population genetics of crypsis in vertebrates: recent insights from
381 mice, hares, and lizards. Heredity. 2019 Aug 9:1-4.

382 Harrison, J.H., 1920. Genetical studies in the moths of the geometrid genus Oporabia (Oporinia)
383 with a special consideration of melanism in the lepidoptera. Journal of Genetics, 9(3),
384 pp.195-280.

385 Haupaix, N., Curantz, C., Bailleul, R., Beck, S., Robic, A. and Manceau, M., 2018. The periodic
386 coloration in birds forms through a prepattern of somite origin. Science, 361(6408),
387 p.eaar4777.

388 Hoekstra, H.E., 2006. Genetics, development and evolution of adaptive pigmentation in
389 vertebrates. Heredity, 97(3), pp.222-234.

390 International Herpetological Society. (2020) *IMPORTANT NOTICE – BANNED MORPHS*. June 19,
391 2020. https://www.ihs-web.org.uk/news/show-news/important-notice-banned-species/

392 Irizarry, K.J. and Bryden, R.L., 2016. In silico analysis of gene expression network components
393 underlying pigmentation phenotypes in the Python identified evolutionarily conserved
394 clusters of transcription factor binding sites. Advances in bioinformatics, 2016.

395 Kelsh, R.N., 2006. Sorting out Sox10 functions in neural crest development. Bioessays, 28(8),
396 pp.788-798.

397 Li, H., Handsaker, B., Wysoker, A., Fennell, T., Ruan, J., Homer, N., Marth, G., Abecasis, G. and
398 Durbin, R., 2009. The sequence alignment/map format and SAMtools. Bioinformatics,
399 25(16), pp.2078-2079.

400 Lister, J.A., Lane, B.M., Nguyen, A. and Lunney, K., 2011. Embryonic expression of zebrafish MiT
401 family genes tfe3b, tfeb, and tfec. Developmental Dynamics, 240(11), pp.2529-2538.

402 Mills, M.G. and Patterson, L.B., 2009, February. Not just black and white: pigment pattern
403 development and evolution in vertebrates. In Seminars in cell & developmental biology
404 (Vol. 20, No. 1, pp. 72-81). Academic Press.

405 McKinnon, J.S. and Pierotti, M.E., 2010. Colour polymorphism and correlated characters:
406 genetic mechanisms and evolution. Molecular ecology, 19(23), pp.5101-5125.

407 Mendel, G. (1866) Versuche u¨ber pflanzen-hybriden. Verhandlungen der naturfoschung
408 Vereins 4, 3–47

409 Oiso, N., Fukai, K., Kawada, A. and Suzuki, T., 2013. Piebaldism. The Journal of Dermatology,
410 40(5), pp.330-335.

411 Olsson, M., Stuart-Fox, D. and Ballen, C., 2013, June. Genetics and evolution of colour patterns
412 in reptiles. In Seminars in cell & developmental biology (Vol. 24, No. 6-7, pp. 529-541).
413 Academic Press.

414 Petratou, K., Subkhankulova, T., Lister, J.A., Rocco, A., Schwetlick, H. and Kelsh, R.N., 2018. A
415 systems biology approach uncovers the core gene regulatory network governing
416 iridophore fate choice from the neural crest. PLoS genetics, 14(10), p.e1007402.

417 Petratou, K., Spencer, S.A., Kelsh, R.N. and Lister, J.A., 2019. The MITF paralog tfec is required in
418 neural crest development for fate specification of the iridophore lineage from a
419 multipotent pigment cell progenitor. bioRxiv, p.862011.

420 Pingault, V., Bondurand, N., Kuhlbrodt, K., Goerich, D.E., Préhu, M.O., Puliti, A., Herbarth, B.,
421 Hermans-Borgmeyer, I., Legius, E., Matthijs, G. and Amiel, J., 1998. SOX10 mutations in
422 patients with Waardenburg-Hirschsprung disease. Nature genetics, 18(2), pp.171-173.

423 Rasys, A.M., Park, S., Ball, R.E., Alcala, A.J., Lauderdale, J.D. and Menke, D.B., 2019. CRISPR-Cas9
424 Gene Editing in Lizards through Microinjection of Unfertilized Oocytes. Cell reports,
425 28(9), pp.2288-2292.

426 Richards, J.R., Yoo, J.H., Shin, D. and Odelberg, S.J., 2019. Mouse models of uveal melanoma:
427 Strengths, weaknesses, and future directions. Pigment Cell & Melanoma Research.

428 Riera, D., 2015. BALL PYTHON GENETICS: MORPH COMBINATIONS TO BE CAUTIOUS OF.
429 https://www.rierareptiles.com/ball-python-genetics-anomalies/

430 Rose, M.P. and Williams, D.L., 2014. Neurological dysfunction in a ball python (Python regius)
431 colour morph and implications for welfare. Journal of Exotic Pet Medicine, 23(3),
432 pp.234-239.

433 Rowan, S., Chen, C.M.A., Young, T.L., Fisher, D.E. and Cepko, C.L., 2004. Transdifferentiation of
434 the retina into pigmented cells in ocular retardation mice defines a new function of the
435 homeodomain gene Chx10. Development, 131(20), pp.5139-5152.

436 San-Jose, L.M. and Roulin, A., 2017. Genomics of coloration in natural animal populations.
437 Philosophical Transactions of the Royal Society B: Biological Sciences, 372(1724),
438 p.20160337.

439 San-Jose, L.M. and Roulin, A., 2018. Toward understanding the repeated occurrence of
440 associations between melanin-based coloration and multiple phenotypes. The American
441 Naturalist, 192(2), pp.111-130.

442 Saenko, S.V., Teyssier, J., Van Der Marel, D. and Milinkovitch, M.C., 2013. Precise colocalization
443 of interacting structural and pigmentary elements generates extensive color pattern
444 variation in Phelsuma lizards. BMC biology, 11(1), p.105.

445 Saenko, S.V., Lamichhaney, S., Barrio, A.M., Rafati, N., Andersson, L. and Milinkovitch, M.C.,
446 2015. Amelanism in the corn snake is associated with the insertion of an LTR-
447 retrotransposon in the OCA2 gene. Scientific reports, 5, p.17118.

448 Saunders, L.M., Mishra, A.K., Aman, A.J., Lewis, V.M., Toomey, M.B., Packer, J.S., Qiu, X.,
449 McFaline-Figueroa, J.L., Corbo, J.C., Trapnell, C. and Parichy, D.M., 2019. Thyroid
450 hormone regulates distinct paths to maturation in pigment cell lineages. Elife, 8,
451 p.e45181.

452 Schweizer, R.M., Durvasula, A., Smith, J., Vohr, S.H., Stahler, D.R., Galaverni, M., Thalmann, O.,
453 Smith, D.W., Randi, E., Ostrander, E.A. and Green, R.E., 2018. Natural selection and
454 origin of a melanistic allele in North American gray wolves. Molecular biology and
455 evolution, 35(5), pp.1190-1209.

456 Sedlazeck, F.J., Rescheneder, P. and Von Haeseler, A., 2013. NextGenMap: fast and accurate
457 read mapping in highly polymorphic genomes. Bioinformatics, 29(21), pp.2790-2791.

458 Steingrímsson, E., Tessarollo, L., Pathak, B., Hou, L., Arnheiter, H., Copeland, N.G. and Jenkins,
459 N.A., 2002. Mitf and Tfe3, two members of the Mitf-Tfe family of bHLH-Zip transcription

460 factors, have important but functionally redundant roles in osteoclast development.
461 Proceedings of the National Academy of Sciences, 99(7), pp.4477-4482.

462 Tachibana, M., Kobayashi, Y. and Matsushima, Y., 2003. Mouse models for four types of
463 Waardenburg syndrome. Pigment cell research, 16(5), pp.448-454.

464 Teyssier J, Saenko SV, Van Der Marel D, Milinkovitch MC. Photonic crystals cause active colour
465 change in chameleons. Nature communications. 2015 Mar 10;6:6368.

466 Ullate-Agote, A., Burgelin, I., Debry, A., Langrez, C., Montange, F., Peraldi, R., Daraspe, J.,
467 Kaessmann, H., Milinkovitch, M.C. and Tzika, A.C., 2020. Genome mapping of a LYST
468 mutation in corn snakes indicates that vertebrate chromatophore vesicles are lysosome-
469 related organelles. Proceedings of the National Academy of Sciences, 117(42),
470 pp.26307-26317.

471 Woodcock, M.R., Vaughn-Wolfe, J., Elias, A., Kump, D.K., Kendall, K.D., Timoshevskaya, N.,
472 Timoshevskiy, V., Perry, D.W., Smith, J.J., Spiewak, J.E. and Parichy, D.M., 2017.
473 Identification of mutant genes and introgressed tiger salamander DNA in the laboratory
474 axolotl, Ambystoma mexicanum. Scientific reports, 7(1), pp.1-10.

475 Wysoker, A., Tibbetts, K. and Fennell, T., 2013. Picard tools version 1.90. http://picard.
476 sourceforge. net (Accessed 14 December 2016), 107(17), p.308.

477

478 **Figures**

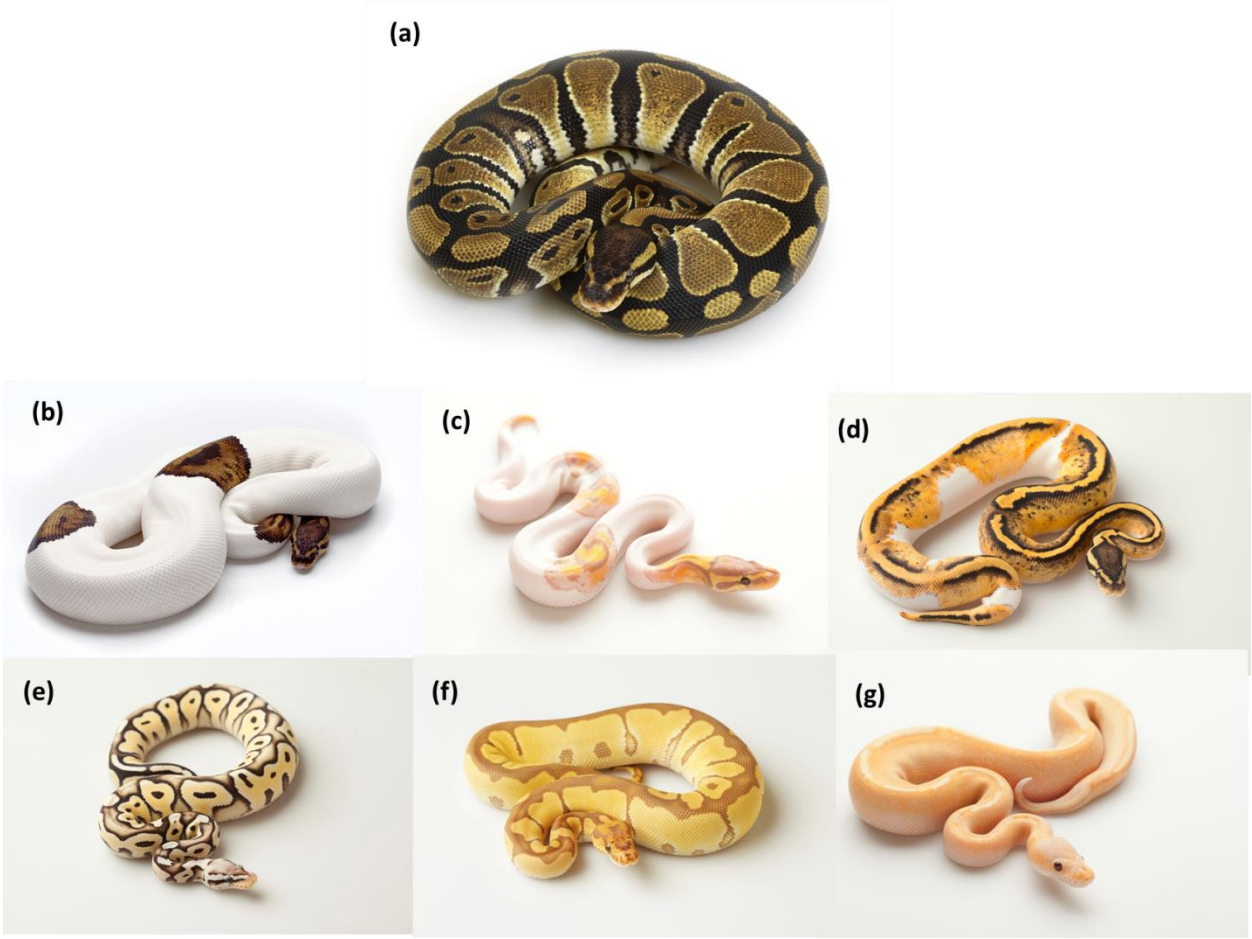

479

480 Figure 1. A small sample of the phenotypic variation found in captive-bred ball pythons (*Python regius*).
481 (a) wild-type, (b) piebald, (c) banana piebald, (d) pastel piebald, (e) pastel HRA enhancer, (f) ultramel
482 clown, (g) banana champagne. Photo credit (b-g): Designing Morphs.

483

484

485

486

487

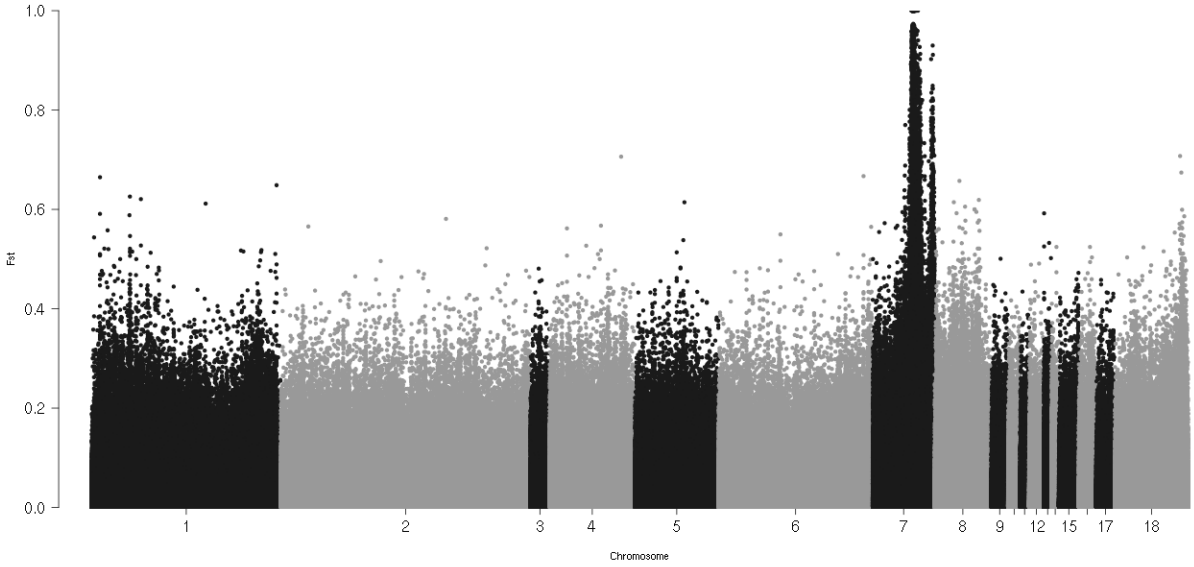

488

489 Figure 2. Fst plot between piebald and non-piebald samples on the chromosome-length assembly
490 (Python_molurus_bivittatus-5.0.2_HiC.assembly).

491

492

5’ GAT ACA CGA GCA 3’
Asp Thr Arg Ala

C>T Arg165

5’ GAT ACA TGA GCA 3’
Asp Thr Stop Ala

493

494 Figure 3. A premature stop codon on Arg165 is the
495 putative causal variant for the piebald phenotype.

496

497

498

499 **Supplementary figures**

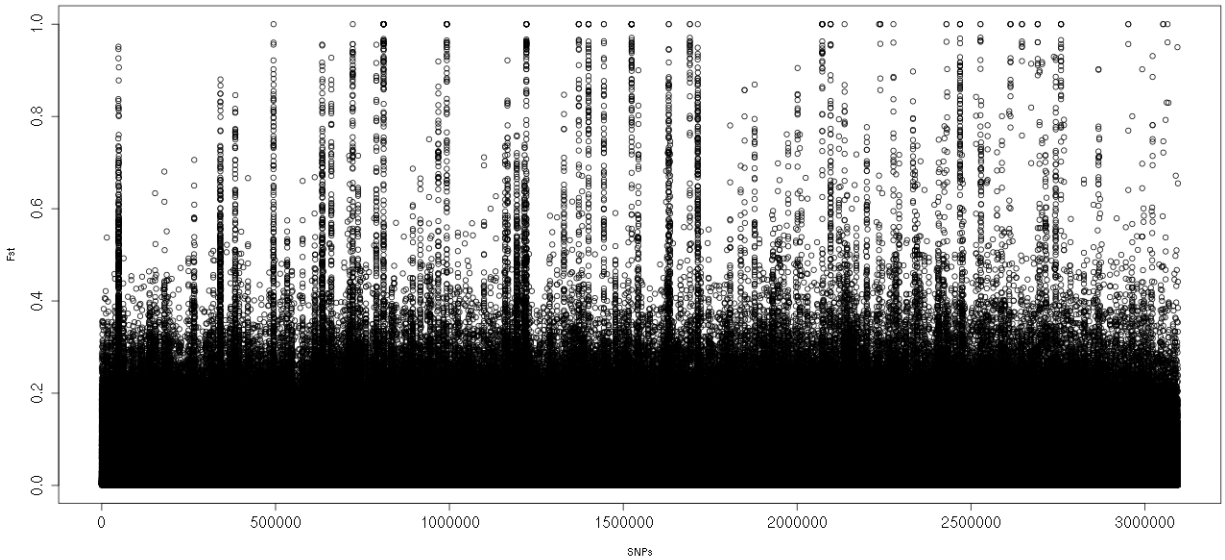

500

501 Figure S1. Fst plot of SNPs mapped to the Burmese python draft assembly (Pmo2.0). The 129 fixed SNPs
502 in this plot were used to map to candidate genes.

503

504

505